Theor Chem Acc (2017) 136:104
DOI 10.1007/s00214-017-2133-8

REGULAR ARTICLE

A molecular electron density theory study of [3 + 2] cycloaddition reactions of chiral azomethine ylides with β-nitrostyrene

Lilia Nasri[1] · Mar Ríos-Gutiérrez[2] · Abdelmalek Khorief Nacereddine[1,3] · Abdelhafid Djerourou[1] · Luis R. Domingo[2]

Received: 20 May 2017 / Accepted: 21 August 2017 / Published online: 6 September 2017

Abstract The molecular mechanism and selectivity of the [3 + 2] cycloaddition (32CA) reaction of a chiral azomethine ylide (AY) with β-nitrostyrene (NS) have been studied within the Molecular Electron Density Theory (MEDT) using DFT methods at the MPWB1K/6-31G(d) computational level. Analysis of the electronic structure of AY indicates that this species has a *pseudodiradical* structure that enables its participation in *pdr-type* 32CA reactions. Analysis of the conceptual DFT reactivity indices allows classifying the AY as a strong nucleophile and NS as a strong electrophile, suggesting a polar process, while Parr functions permit to predict a high regioselectivity. The 32CA reaction presents a relatively low activation enthalpy, 4.1 kcal·mol^{-1}, and is completely regio- and stereoselective. ELF topological analysis allows characterising the molecular mechanism of these *pdr-type* 32CA reactions as a non-concerted *two-stage one-step* mechanism, the reaction being classified as a [2n + 2τ] process.

Keywords Azomethine ylide · [3 + 2] cycloaddition · Selectivity · MEDT · Mechanism · DFT calculations · NCI analysis

Electronic supplementary material The online version of this article (doi:10.1007/s00214-017-2133-8) contains supplementary material, which is available to authorized users.

✉ Mar Ríos-Gutiérrez
rios@utopia.uv.es

✉ Abdelmalek Khorief Nacereddine
khorief.abdelmalek@univ-annaba.org

[1] Laboratoire de Synthèse et Biocatalyse Organique, Département de Chimie, Faculté des Sciences, Université Badji Mokhtar Annaba, BP 12, 23000 Annaba, Algeria

[2] Department of Organic Chemistry, University of Valencia, Dr. Moliner 50, E-46100 Burjassot, Valencia, Spain

[3] Département de Physique et Chimie, Ecole Normale Supérieure d'Enseignement Technologique de Skikda, Azzaba, Skikda, Algeria

1 Introduction

Imidazolidine **1** and its derivatives (Scheme 1) are a class of versatile heterocyclic compounds that can be found in many natural products [1]. They exhibit a large variety of biological and pharmacological activities, such as herbicides, fungicides, anti-allergy, anti-tumour, anti-inflammatory, anti-bacterial, antioxidant and analgesic activities [2]. In addition, compounds containing a pyrrolidine ring **2** are components of natural substances that attract a keen interest from the viewpoint of medicinal chemistry due to their broad spectrum of pronounced biological activity [3–5]. The link of two different bioactive molecules with complementary pharmacophoric functions has often shown synergistic effects. Therefore, the combination of both imidazolidine **1** and pyrrolidine **2** in the same molecule may produce a new group of compounds, hexahydro-1*H*-pyrrolo [1,2-*c*] imidazoles **3** (see Scheme 1), with enhanced or poly-biological activities widely applied in pharmacy and medicine due to their versatile biological properties [6, 7].

[3 + 2] cycloaddition (32CA) reactions are one of the most attractive synthetic methods for the construction of five-membered heterocyclic compounds [8]. The 32CA reaction of azomethine ylide (AY) **4** with ethylene **5** is an appealing alternative tool for the construction of hybrid heterocycles containing pyrrolo imidazole **3** subunits of pharmacological importance (see Scheme 2). [9]

Recent Molecular Electron Density Theory (MEDT) [10] studies devoted to 32CA reactions have allowed establishing a very good correlation between the electronic structure of

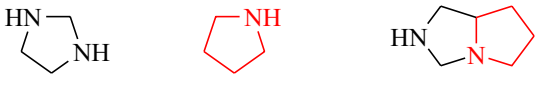

1 2 3

Scheme 1 Structures of imidazolidine **1**, pyrrolidine **2** and pyrrolo imidazole **3**

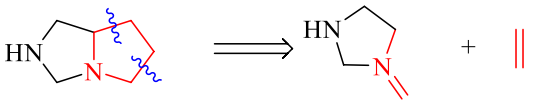

3 4 5

Scheme 2 Retrosynthesis of pyrrolo imidazole **3**

three-atom-components (TACs) and their reactivity towards ethylene **5** [11, 12]. Thus, depending on the electronic structure of the TAC, the non-polar 32CA reactions have been classified into *pseudodiradical*-type (*pdr-type*) [11, 12], *pseudoradical*-type (*pmr-type*) [12], carbenoid-type (*cb-type*) [13] and zwitterionic-type (*zw-type*) [11] reactions.

The reactivity trend decreases in the following order: *pseudodiradical* > *pseudoradical* > carbenoid > zwitterionic, in such a manner that while *pdr-type* 32CA reactions take place easily through earlier transition state structures (TSs) even with a very low polar character [11, 12], *zw-type* 32CA reactions demand adequate nucleophilic/electrophilic activations to take place. In general, AYs are very strong nucleophiles, reacting very quickly with either species containing a multiple bond, both in non-polar and polar *pdr-type* 32CA reactions [14, 15].

Recently, the 32CA reaction between AY **6** and β-nitrostyrene (NS) **7** was theoretically studied at the ωB97XD/6-31G(d) computational level (Scheme 3). [16] Interestingly, this reaction proceeds through a polar mechanism in which the formation of a hydrogen bond between one nitro oxygen of NS **7** and the AY N–H hydrogen of **6** is responsible for the *meta/endo* selectivity leading to the formation of spiro[pyrrolidin-2,3′]oxindole **8a** as the major cycloadduct, as experimentally found.

One experimental example of the synthesis of heterocycles containing pyrrolo imidazole **3** subunits is the multicomponent reaction (MCR) between 2-tert-butyl-3-methylimidazolidin-4-one **9**, benzaldehyde **10** and NS **7**, in the presence of triethylamine as base, recently reported by Zhang et al. [17] (Scheme 4). This one-pot reaction yields pyrrolo [1,2-e] imidazol-1-one **12n-a** as single product, with high yield (99%) and high diastereoselectivity (up to 98:2), through a 32CA reaction of AY **11a**, generated in situ from the condensation of **9** and **10**, with NS**7**.

Our research program is focused on the study of the molecular mechanisms and the origin of the experimental selectivity of cycloaddition reactions within MEDT [18–20]. Herein, we present a MEDT investigation of the molecular mechanism of the 32CA reaction of AY **11a** with NS **7**, providing a rationalisation of the regio- and stereoselectivity experimentally found by Zhang et al. [17]. To this end, the 32CA reaction involving the simpler 2-methyl-3-methylimidazolidin-4-one **11b**, in which the bulky *t*-Bu group was replaced by a methyl group, which was selected as a reduced model of the experimental reaction involving AY

Scheme 3 32CA reaction between 3-(benzylideneamino) oxindole **6** and NS **7**

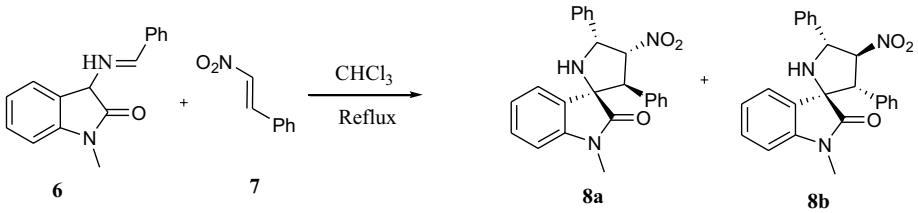

6 7 8a 8b

15:1

Scheme 4 MCR between imidazolidinone **9**, benzaldehyde **10** and NS **7** affording pyrrolo imidazole **12n-a**

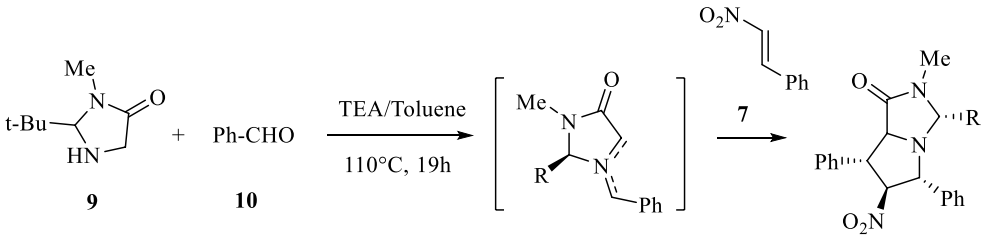

9 10

11a R = t-Bu
11b R = Me
in situ

12n-a R = t-Bu
12n-b R = Me

11a. The reactivity of these substituted AYs in 32CA reactions is analysed.

2 Computational methods

DFT calculations were performed using the MPWB1K functional [21] together with the 6-31G(d) basis set [22]. This functional has been recently used in the study of 32CA reactions [12, 13]. Further single point energy calculations at the MPWB1K/6-311G(d,p)//MPWB1K/6-31G(d) level not produced noticeable changes in relative energies (see Supplementary Material). Optimisations were carried out using the Berny analytical gradient optimisation method [23, 24]. The stationary points were characterised by frequency computations in order to verify that TSs have one and only one imaginary frequency. The IRC paths [25] were traced in order to check the energy profiles connecting each TS to the two associated minima of the proposed mechanism using the second order González–Schlegel integration method [26, 27]. Implicit solvent effects of toluene were considered through single point energy calculations using the polarisable continuum model (PCM) developed by Tomasi group [28, 29] in the framework of the self-consistent reaction field (SCRF) [30–32]. Enthalpies, entropies and Gibbs free energies in toluene were calculated with standard statistical thermodynamics at 110 °C and 1 atm from the optimised gas phase structures [22]. CDFT global reactivity indices [33, 34] and Parr functions [34] were computed using the equations given in reference [34]. The global electron density transfer [35] (GEDT) is computed by the sum of the natural atomic charges (q), obtained by a natural population analysis (NPA) [36, 37], of the atoms belonging to each framework (f) at the TSs; GEDT = Σq_f. All computations were carried out using the Gaussian 09 suite of programs [38].

ELF [39], QTAIM [40] and NCI [41] studies were performed with the TopMod [42], Multiwfn [43] and NCIplot [44] programs, respectively, using the corresponding MPWB1K/6-31G(d) mono determinantal wave functions. A bonding evolution theory (BET) [45] procedure was used for the characterisation of the bond formation processes of the new C–C single bonds by performing the topological analysis of the ELF, over a grid spacing of 0.1 a.u., for 673 nuclear configurations along the corresponding IRC path.

3 Results and discussion

The present theoretical study has been divided into four parts: (1) first, the electronic structures of the simplest AYs **14** and the methyl-substituted AY **11b** are characterised and compared by ELF and NPA analyses in order to understand the reactivity of these TACs; (2) in the second part, the CDFT reactivity indices of the reagents are analysed in order to predict their reactivity in these 32CA reactions; (3) third, an analysis of the reaction paths associated with the 32CA reactions of AYs **11a**,**b** with NS **7** is performed with the aim of reproducing and explaining the experimental selectivity; and (4) finally, an ELF topological analysis of formation of the new C–C single bonds is carried out.

3.1 ELF and NPA characterisation of the electronic structures of AYs 11b and 14

In order to characterise the electronic structure of the experimental AY **11a** and thus, to predict its reactivity in 32CA reactions, an ELF [39] topological analysis of the simplest AY **14** and the simpler experimental model AY **11b** were first performed. ELF attractors, including the most representative valence basin populations and natural atomic charges, ELF basins and the proposed ELF-based Lewis structures are shown in Fig. 1.

Due to the symmetry of the simplest AY **14**, ELF topological analysis of this TAC shows a symmetrical distribution of the electron density. Thus, while one V(C, N) disynaptic basin is observed in the two C–N bonding regions with an electron population of 2.58e, a pair of V(C) and V'(C) monosynaptic basins, integrating a total population of 1.03e, is present at both terminal carbons. Consequently, ELF topology of AY **14** indicates that this TAC has a *pseudodiradical* electronic structure that enables its participation in *pdr-type* 32CA reactions. It should be emphasised that the presence of two V(C) monosynaptic basins characterising a *pseudoradical* carbon centre is the consequence of the planar arrangement, i.e. sp^2 hibridisation, around the corresponding carbon atom.

On the other hand, although the substitution at AY **11b** breaks the molecular symmetry, topological analysis of the ELF of this TAC shows a similar electronic structure to that of the simplest AY **14**. One V(C1) monosynaptic basin, integrating 0.59e, and two V(C3) and V'(C3) monosynaptic basins, integrating a total population of 0.61e, are observed at the C1 and C3 carbons, thus characterising two C1 and C3 *pseudoradical* centres, while the two C1–N2 and N2–C3 bonding regions appear described by two V(C1, N2) and V(N2, C3) disynaptic basins with populations of 2.46e and 2.97e. The substitution at AY **11b** has not only provoked a decrease of the electron density of the two C1 and C3 *pseudoradical* centres as a consequence of the delocalisation of part of their electron density towards the carbonyl and phenyl substituents, respectively, but also a slight pyramidalisation of C1 due to the ring tension so that only one V(C1) monosynaptic basin appears. Despite these small topological differences relative to AY **14**, AY **11b** also presents a *pseudodiradical* electronic structure that enables its participation in *pdr-type* 32CA reactions. The lower electron density

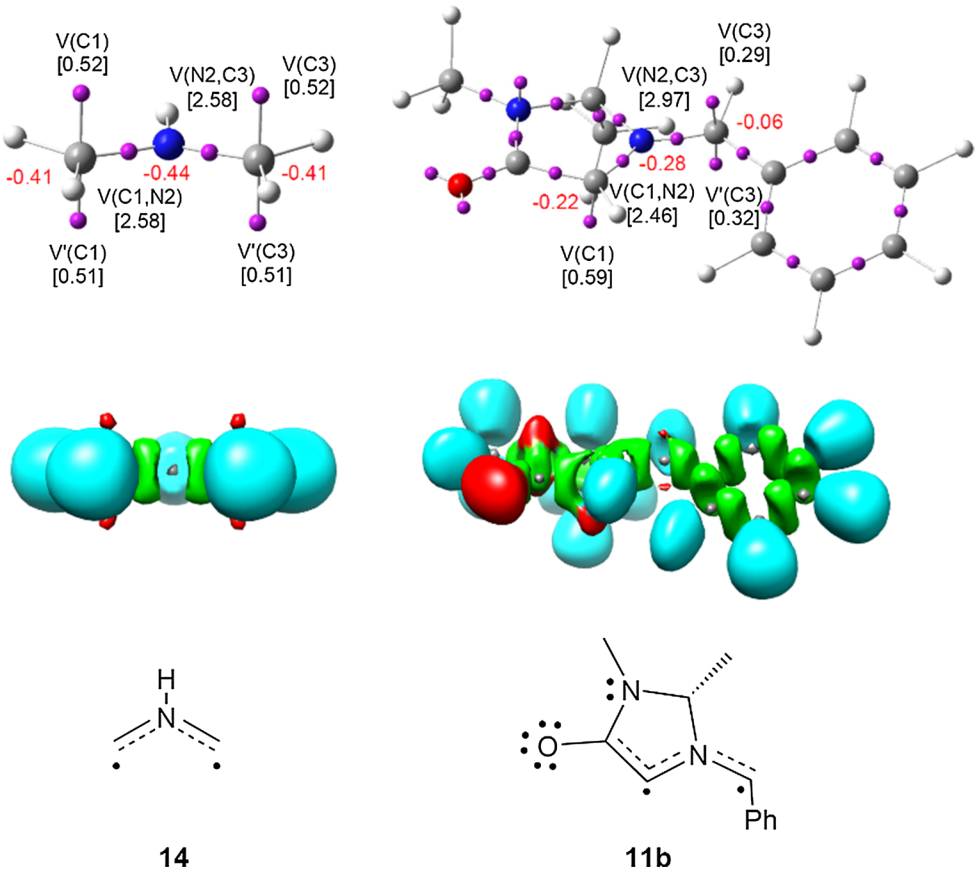

Fig. 1 ELF attractors together with some valence basin populations and natural atomic charges (negative in *red*, positive in *blue* and neutral in *green*), in average number of electrons (e), ELF basins, represented at iso values of 0.80 (**14**) and 0.74 (**11b**) a.u., and the proposed Lewis structures for AYs **14** and **11b**

populations of the V(C1) and V(C3) monosynaptic basins found in AY **11b** with respect to those found in the simplest AYs **14** may suggest a lower reactivity of the former.

Once the bonding pattern of these TACs was established, the charge distribution was analysed through an NPA. Natural atomic charges of the more relevant atoms are included in Fig. 1. NPA of both AYs reveals that the three C1, N2 and C3 atoms are negatively charged. While in AY **14,** the negative charges of these three atoms are relatively high and very similar, ca. -0.4e, in AY **11b,** the C1 and N2 atoms have been depopulated to −0.22e and −0.28e, and the negative charge of the C3 carbon has notably decreased to a negligible value of −0.06e. Consequently, this charge distribution allows ruling out the common representation of AYs as 1,2-zwitterionic Lewis structures in which a positive charge and a negative charge are entirely localised at the N2 nitrogen and at the C3 carbon, respectively.

3.2 Analysis of the CDFT reactivity indices of the reagents AYs 11a,b and NS 7

Numerous studies devoted to polar organic reactions have proven that the analysis of the reactivity indices defined within the CDFT [33, 34] is an effective tool to understand the reactivity of the reagents involved in polar cycloaddition reactions. Global CDFT indices, i.e. the electronic chemical potential [46, 47], μ, the chemical hardness [46, 47], η, the electrophilicity [48], ω, and the nucleophilicity [49, 50], *N*, at the ground state of the reagents, were computed according to the equations given in [34] and are displayed in Table 1.

Analysis of the μ of the reagents provides information only about the direction of the GEDT flux along a polar reaction. The electronic chemical potentials μ of AY **11a** and **11b**, −3.06 and −3.09 eV, are higher than that of NS **7**, −4.78 eV. Thereby, along a polar reaction, the GEDT will flux from AYs **11a**,**b** to NS **7**, in clear agreement with the GEDT computed at the TSs (see later).

Table 1 Global MPWB1K/6-31G(d) electronic chemical potential (μ), chemical hardness (η), electrophilicity (ω) and nucleophilicity (*N*), in eV, of ethylene **5**, AYs **11a**,**b** and **14**, and NS**7**

Compound	μ	η	ω	*N*	*pr*
NS **7**	−4.78	6.27	1.82	2.62	
AY **11b**	−3.09	4.73	1.01	5.08	1.07
AY **11a**	−3.06	4.67	1.00	5.14	1.10
Ethylene **5**	−3.38	10.05	0.57	1.83	
AY **14**	−1.70	6.34	0.23	5.36	0.84

The electrophilicity ω and nucleophilicity *N* indices of simplest AY **14** are 0.23 and 5.36 eV, being classified as a marginal electrophile and as a strong nucleophile based on the electrophilicity [51] and nucleophilicity [52] scales defined employing the MPWB1K functional. Substitution at one terminal carbon and at the nitrogen atom notably increases the electrophilicity ω index to 1.00 (**11a**) and 1.01 (**11b**) eV and slightly decreases the nucleophilicity *N* index to 5.14 (**11a**) and 5.08 (**11b**) eV, both being classified at the border line of strong electrophiles but remaining strong nucleophiles. Note that the *t*-Bu substituent of **11a** has no significant impact on the electronic features of **11b**, supporting the choice of **11b** as a representative reduced model of **11a**. Thus, in a polar organic reaction, both AYs **11a**,**b** will behave as strong nucleophiles, showing a very similar reactivity.

Polar cycloaddition reactions require the participation of good electrophiles and good nucleophiles [53, 54]. Ethylene **5** is one of the poorest electrophilic, ω = 0.57 eV, and nucleophilic, *N* = 1.83 eV, species involved in cycloaddition reactions, being classified as a marginal electrophile and a marginal nucleophile. Consequently, ethylene **5** cannot participate in polar reactions. The inclusion of a phenyl substituent at one carbon of ethylene **5** and a nitro group at the other one strongly increases the electrophilicity ω and nucleophilicity *N* indices of NS **7** to 1.82 and 2.62 eV, respectively, being classified as a strong electrophile and as a moderate nucleophile. Therefore, NS **7** will behave as a strong electrophile when facing the strongly nucleophilic AYs **11a**,**b**, and accordingly, it is expected that the 32CA reaction between them will proceed via a polar mechanism with low activation energy.

In order to characterise the participation of TACs in *pdr-type* 32CA reactions, the *pr* index has recently been introduced [11, 12]. TACs with *pr* values higher than 0.90 participate in *pdr-type* 32CA reactions and can be related to species having a very soft character, i.e. with low hardness η values, and a low ionisation potential, i.e. with high nucleophilicity *N* values, while TACs with low *pr* values do not participate in *pdr-type* 32CA reactions [16]. AYs **14** and **11a**,**b** have *pr* values of 0.84 (**14**), 1.07 (**11a**) and 1.10 (**11b**), indicating that these TACs will exhibit high *pdr-type* reactivity [11, 12], in clear agreement with their *pseudodiradical* character revealed by the topological analysis of the ELF (see Fig. 1).

In order to predict the most favourable initial electrophile/nucleophile two-centre interaction in these 32CA reactions, the electrophilic P_k^+ Parr functions of NS **7** and the nucleophilic P_k^- Parr functions of AYs **11a**,**b** were analysed [55]. The 3D representations of the Mulliken atomic spin density (ASD) of the radical cations **11a**$^{\cdot+}$and **11b**$^{\cdot+}$, and of radical anion **7**$^{\cdot-}$, together with the nucleophilic P_k^- Parr functions of AYs **11a**,**b** and the electrophilic P_k^+ Parr functions of NS **7** are given in Fig. 2.

Analysis of the nucleophilic P_k^- Parr functions of AYs **11a**,**b** indicates that they are mainly gathered at the two AY C1 and C3 carbons (see Scheme 5 for atom numbering), the former being twice as nucleophilically activated as the latter, $P_{C1}^- = 0.64$ and $P_{C3}^- = 0.35$ at **11a**, and $P_{C1}^- = 0.63$ and $P_{C3}^- = 0.37$ at **11b**, while the N2 nitrogen is nucleophilically deactivated, $P_{N2}^- = -0.16$ (**11a**) and −0.17 (**11b**). On the other hand, the electrophilic P_k^+ Parr functions of NS**7** indicate that the C5 carbon atom is the most electrophilic centre of this molecule, $P_{C5}^+ = 0.27$, the C4 carbon presenting a negligible electrophilic activation, $P_{C4}^+ = 0.08$.

Consequently, the most favourable initial nucleophile/electrophile interaction along the 32CA reactions of AYs **11a**,**b** with NS **7** will occur between the most nucleophilic centre of AYs **11a**,**b**, the C1 carbon, and the most electrophilic centre of NS**7**, the C5 carbon. Furthermore, the great differences between the nucleophilic P_{C1}^- and P_{C3}^- Parr functions of AYs **11a**,**b** and between the electrophilic P_{C4}^+ and P_{C5}^+ Parr functions of NS **7** clearly suggest a high regioselectivity, in good agreement with the experimental outcomes.

3.3 Energy profile and geometry analyses

Due to the chiral character of AYs **11a**,**b** and the non-symmetry of NS **7**, the 32CA reactions of AYs **11a**,**b** with NS

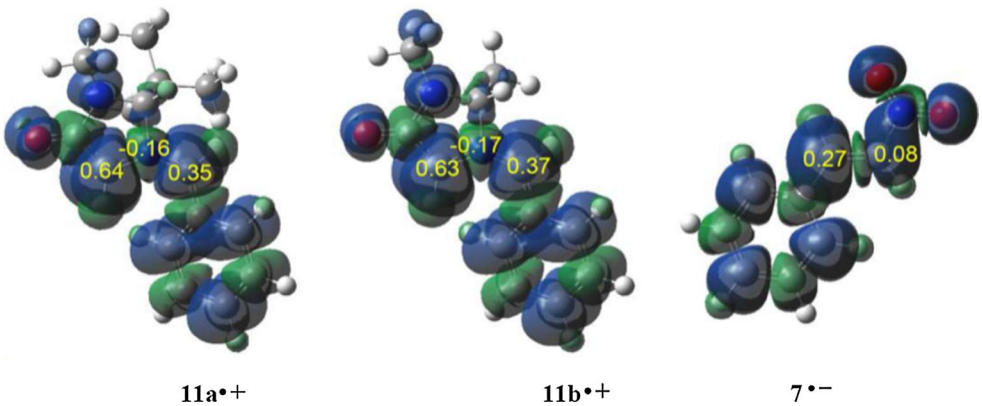

Fig. 2 3D representation of the Mulliken ASD of radical cations **11a**$^{\cdot+}$ and **11b**$^{\cdot+}$and radical anion **7**$^{\cdot-}$, including the nucleophilic P_k^- Parr functions of AYs **11a**,**b** and the electrophilic P_k^+ Parr functions of NS **7**

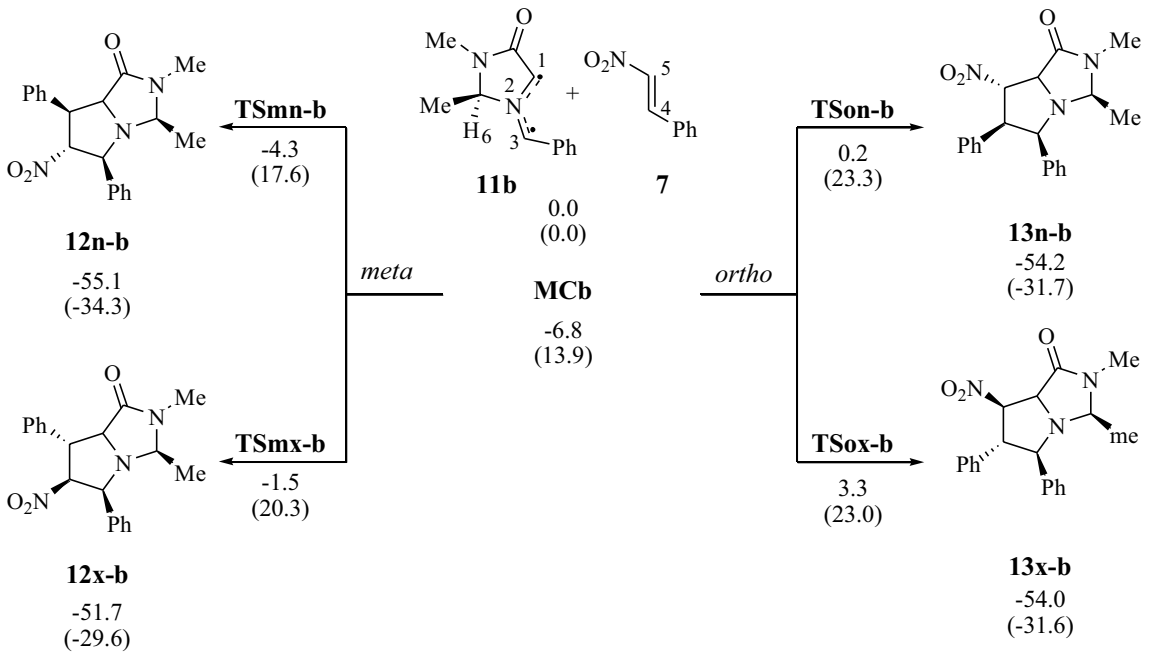

Scheme 5 Regio- and stereoisomeric channels associated with the *anti* pathways for the 32CA reactions of AY **11b** with NS **7**. Relative enthalpies and Gibbs free energies, in parentheses, are given in kcal·mol^{-1}

7 can proceed via eight competitive channels, namely two regioisomeric (*ortho* and *meta*), two stereoisomeric (*endo* and *exo*) and two diastereofacial (*syn* and *anti*) channels. The *ortho* and *meta* nomenclature is related to the C1–C4 and C1–C5 interactions, respectively, the *endo* and *exo* terminology is associated with the approach of the nitro group of NS**7** towards or away from the N2 nitrogen of the AY C1–N2–C3 bent framework, respectively, while the *syn* and *anti* terms correspond to the approach of NS**7** towards the two diastereotopic faces of AYs **11a**,**b** defined by the R– group present in the imidazolidine ring. Due to the high steric hindrance provoked by the *t*-Bu group of **11a**, only the *anti* diastereofacial approach modes were considered for the present study.

*3.3.1 32CA reaction of methyl-substituted AY **11b** with NS **7***

The 32CA reaction of the simpler AY **11b** with NS **7** takes place through a one-step mechanism as the reagents, AYs **11b** and NS **7**, one TS, **TSmn-b**, **TSmx-b**, **TSon-b** and **TSox-b**, and the corresponding cycloadduct, **12n-b**, **12x-b**, **13n-b** and **13x-b**, were located and characterised along each one of the four competitive *anti* stereoisomeric pathways (see Scheme 5). Relative enthalpies and Gibbs free energies are given in Scheme 5.

As can be seen in Scheme 5, two of the four TSs are found below the separated reagents considering enthalpies; however, when the formation of a molecular complex (MC), **MCb**, which is strongly stabilised by 6.8 kcal·mol^{-1} with respect to the separated reagents, is considered, the activation enthalpies associated with the 32CA reaction between AY **11b** and NS **7** become 2.5 (**TSmn-b**), 5.3 (**TSmx-b**), 7.1 (**TSon-b**) and 10.1 kcal·mol^{-1} (**TSox-b**). On the other hand, reaction energies are very similar, ranging from −44.8 (**12x-b**) to −48.3 (**12n-b**) kcal·mol^{-1}.

Some appealing conclusions can be drawn from these energy results: (1) the 32CA reaction between AY **11b** and NS **7** presents a relatively low activation enthalpy, 2.5 kcal·mol^{-1}, in reasonable agreement with the high nucleophilic and electrophilic character of the reagents as well as with the suggested *pdr-type* reactivity of **11b** (see Sect. 3.1); (2), the activation enthalpy associated with **TSmn-b** is 5.5 kcal·mol^{-1} lower than that associated with the non-polar 32CA reaction of AY **11b** with ethylene **5**, 8.0 kcal·mol^{-1}, thus suggesting that the electrophilic activation of the ethylene favours the reaction; (3) the reaction is completely *meta* regioselective and highly *endo* stereoselective as the most favourable **TSmn-b** is 4.6 kcal·mol^{-1} below *ortho* **TSon-b** and 2.8 kcal·mol^{-1} below *exo* **TSmx-b**; and (4) when entropies are added to the enthalpies, Gibbs free energies increase by between 19.8 and 23.0 kcal·mol^{-1}. Thus, the activation Gibbs free energy via **TSmn-b** reaches 17.6 kcal·mol^{-1}, while the formation of the corresponding cycloadduct becomes exergonic by −34.3 kcal·mol^{-1}. The strong exergonic character of the reaction, ca. 31 kcal·mol^{-1}, makes this 32CA reaction irreversible. Therefore, this 32CA reaction is under kinetic control only; and (5) accordingly,

a stereoisomeric mixture of *meta* cycloadducts **12n-b** and **12x-b**, in which the *endo* is obtained as the major product, will be kinetically expected for this reaction model.

The geometries of the TSs involved in the 32CA reaction of AY **11b** with NS **7**, including the distances between the interacting carbon atoms, are shown in Fig. 3. The distances between the two C1 and C5 interacting carbons indicate that the more favourable *meta* TSs are geometrically asynchronous, while the *ortho* ones are practically synchronous. Interestingly, **TSmx-b** is slightly more asynchronous than the most favourable **TSmn-b**. In addition, at the *meta* TSs, the distances involving the C5 carbon, which corresponds to the most electrophilic centre of AY **11b** (see Sect. 3.2), are clearly shorter. Therefore, an asynchronous bond formation process in which the C1–C5 bond formation is more advanced than the C3–C4 one can be expected along the more favourable *meta* regioisomeric pathways, in agreement with the previous analysis of the local reactivity by the Parr functions. It is also noteworthy to emphasise that the short distances between one of the oxygen atoms of the nitro group of NS **7** and the H6 or C1–H acidic hydrogens of AY **11b** at the *endo* and *exo* TSs, respectively, i.e. 2.25 Å (**TSmn-b**), 2.53 Å (**TSmx-b**), 2.28 Å (**TSon-b**) and 2.61 Å (**TSox-b**), suggest the presence of stronger O···H hydrogen bonds (HB) at the *endo* TSs than at the *exo* ones.

Numerous studies have shown a strong relationship between the polar character and the feasibility of organic reactions; [16] the larger the GEDT at the TS is, the more polar and thus, faster, the reaction. In order to evaluate the electronic nature, i.e. polar or non-polar of the 32CA reaction between AY **11b** and NS **7**, the GEDT at the TSs was analysed [35]. The GEDT that fluxes from the nucleophilic AY framework towards the electrophilic NS one at the TSs (see Fig. 3) indicates that the 32CA reaction between AY **11b** and NS **7** has a considerable polar character, according to the high nucleophilicity of AY **11a** and the high electrophilicity of NS **7**, and account for the complete *meta* regioselectivity predicted by the Parr functions.

*3.3.1.1 32CA reaction of t-Bu substituted AY **11a** with NS **7*** Although the *t*-Bu group of AY **11a** does not produce significant changes in the electronic reactivity of the methyl-substituted AY **11b** (see Sect. 3.2), taking into account that Zhang et al. obtained *meta/endo/anti* pyrrolo imidazole **12n-a** as a single stereoisomer (see Scheme 4) instead of a *meta/anti* **12n-a**:**12x-a** product mixture, the *endo/exo* stereoisomeric channels associated with the *meta/anti* reaction paths of the experimental 32CA reaction of AY **11a** with NS**7** were further studied in order to reproduce and explain the complete *endo* stereoselectivity experimentally observed.

Along the *meta/anti* pathways associated with the 32CA reaction between AY **11a** and NS **7**, the reagents, two TSs, **TSmn-a** and **TSmx-a**, and two cycloadducts, **12n-a** and **12x-a**, were located and characterised. Consequently, this reaction also takes place through a one-step mechanism (see

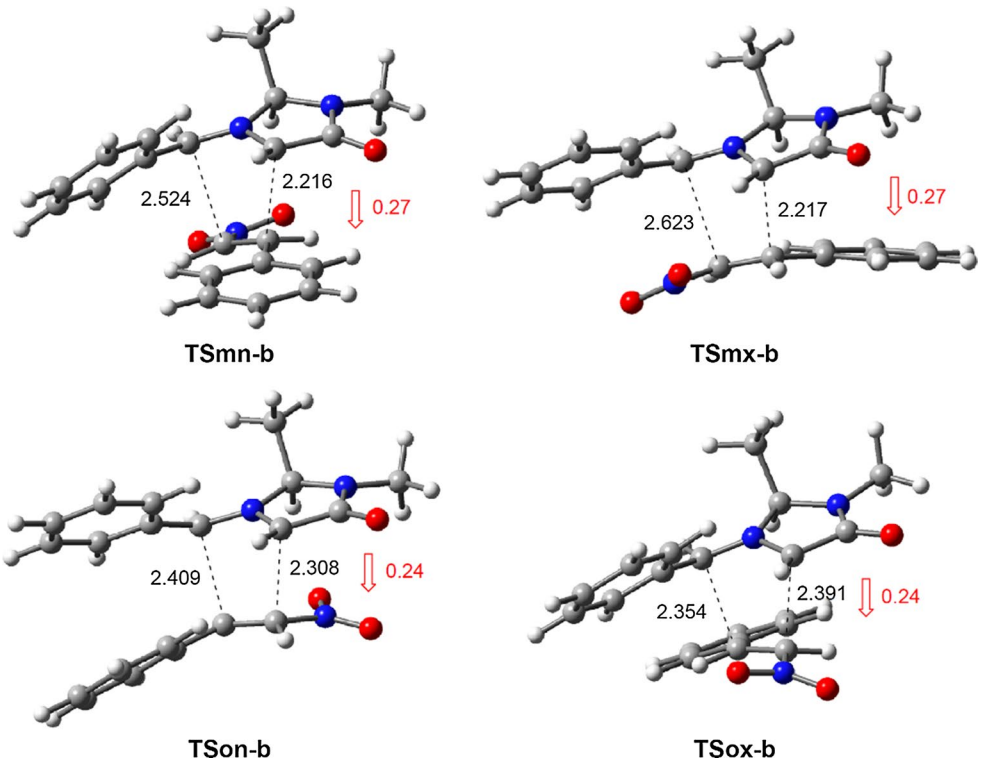

Fig. 3 MPWB1K/6-31G(d) geometries of the TSs involved in the 32CA reaction between AY **11b** and NS **7**. GEDT values, in *red*, are given in average number of electrons, e

Scheme 6). Relative enthalpies and Gibbs free energies are given in Scheme 6.

As in the 32CA reaction involving AY **11b**, the TSs are found below the separated reagents. However, considering the formation of an MC, **MCa**, stabilised by 8.8 kcal·mol^{-1}, the activation enthalpies associated with **TSmn-a** and **TSmx-a** become 4.1 and 7.3 kcal·mol^{-1}, the reaction being strongly exothermic, −48.4 (**12n-a**) and −43.7 (**12x-a**). The most notable energy change in comparison with the enthalpy profile involving the methyl-substituted counterpart **11b** is the increase of the activation enthalpy related to the more favourable **TSmn-a** by only 1.7 kcal·mol^{-1}, which is significant enough to increase the energy difference between the *endo/exo* pair of **TSmn-a** and **TSmx-a** to 3.2 kcal·mol^{-1}. Note that the similar electronic behaviour of both AYs **11a** and **11b** as strong nucleophiles towards the strongly electrophilic NS **7** accounts for this low energy difference between **TSmn-a** and **TSmn-b**. When entropies are added to the enthalpies, Gibbs free energies increase by between 18.6 and 22.2 kcal·mol^{-1}. Now, a total *endo* stereoselectivity is expected as **TSmn-a** is 4.6 kcal·mol^{-1} more stable than **TSmx-a**, in complete agreement with the experimental attainment of *meta/endo* pyrrolo imidazole **12n-a** as a single stereoisomer. The strong exergonic character of the reaction, 36 kcal·mol^{-1}, makes this 32CA reaction irreversible.

The geometries of the TSs involved in the 32CA reaction of AY **11a** with NS **7**, including the distances between the interacting carbon atoms, are represented in Fig. 4. The distances between the interacting carbons, which are very similar to those at the *meta* TSs associated with the 32CA reaction involving AY **11b**, indicate that these *meta* TSs are also asynchronous, the C1–C5 bond formation being more advanced than the C3–C4 one. **TSmx-a** remains more asynchronous than the more favourable **TSmn-a**. The great similarity between the geometries of these TSs and those of the *meta* TSs related to the reaction involving AY **11b** accounts for the similar reactivity of both AYs anticipated by the analysis of the CDFT reactivity indices (Sect. 3.2). Accordingly, also short distances between one of the oxygen atoms of the nitro group of NS**7** and the AY H6 (*endo*) or C1–H (*exo*) acidic hydrogens can be found, 2.39 and 2.29 Å, suggesting the presence of O···H HBs.

The high GEDT that fluxes from the nucleophilic AY framework towards the electrophilic NS one (see Fig. 4), which is very similar to that found at **TSmn-b** and **TSmx-b** due to the similar electronic behaviour of both AYs **11a**,**b** as strong nucleophiles, emphasise the equally high polar character of the 32CA reaction of AY **11a** with NS **7**.

3.3.2 *Origin of the endo selectivity in the 32CA reactions of AYs **11a**,**b** with NS **7***

As the reagents approach each other along a polar reaction, there is an electron density transfer from the nucleophilic towards the electrophilic frameworks, in such a manner that while the former somehow loses electron density, thus being positively charged, the latter somehow gathers electron density, being negatively charged.

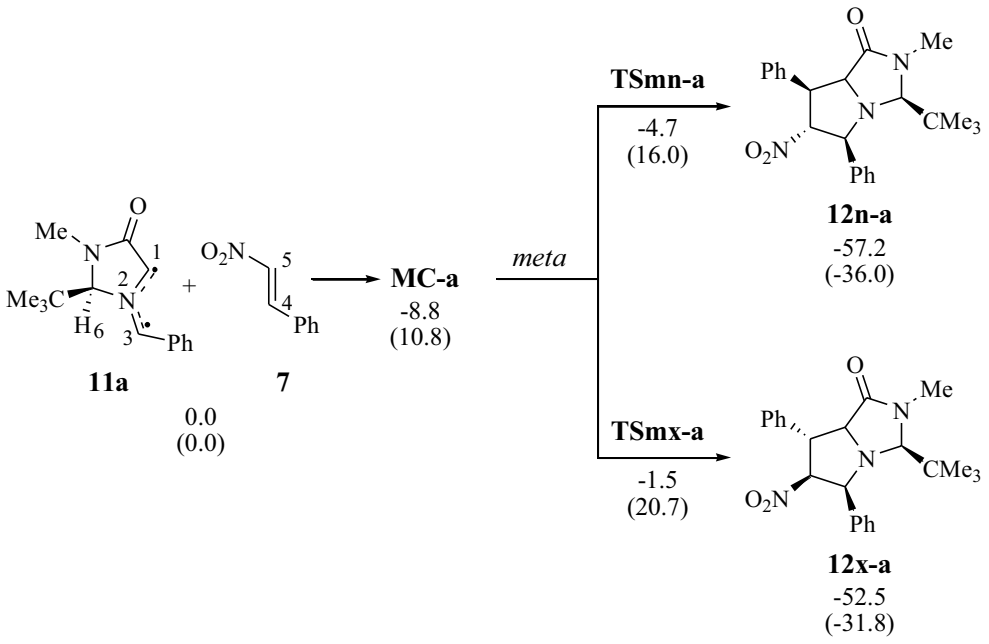

Scheme 6 *Endo* and *exo* stereoisomeric channels associated with the *meta/anti* pathways for the 32CA reactions of AY **11a** with NS **7**. Relative enthalpies and Gibbs free energies, in parentheses, are given in kcal·mol^{-1}

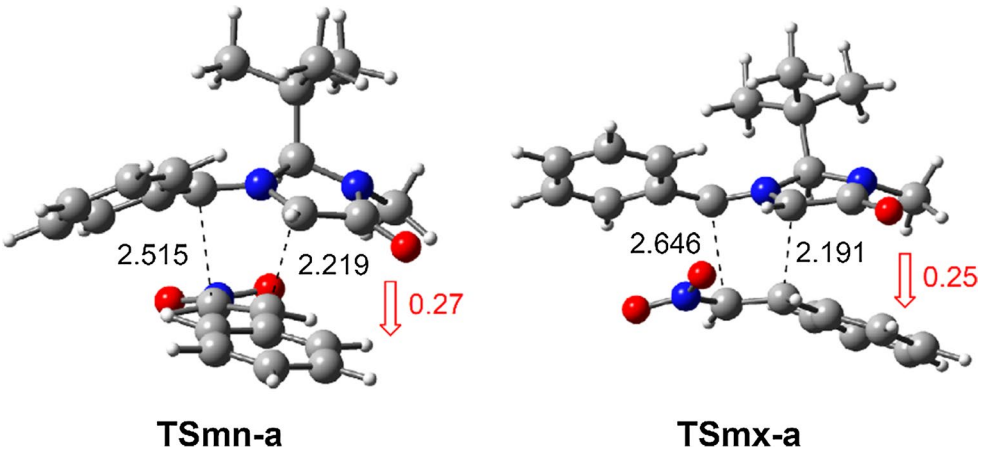

Fig. 4 MPWB1K/6-31G(d) geometries of the *meta* regioisomeric TSs involved in the 32CA reaction between AY **11a** and NS **7**. GEDT values, in *red*, are given in average number of electrons, e

The high GEDT taking place at the more favourable *meta* **TSmn-a** and **TSmx-a** causes these TSs to have a strong zwitterionic character, which is evidenced by an analysis of their molecular electrostatic potential (MEP). Figure 5 shows the MEPs of the reagents as well as *endo* **TSmn-a** and *exo* **TSmx-a**. As can be seen, the C3–H and H6 hydrogen atoms of AY **11a** gather the more intense blue region (positive charge) of the MEP of this TAC, while the MEP region around the nitro group of NS**7** is the reddest (negative charge) within this molecule. Interestingly, at both TSs the intensity of the blue and red colours of the MEP around the C3–H and H6 hydrogens, and the nitro group, respectively, is stronger, as a consequence of the GEDT process.

At the *endo* **TSmn-a**, the nucleophilic AY and electrophilic NS fragments are orientated in such a manner that the C3–H and H6 hydrogens are situated above the electron-withdrawing nitro group, while at the *exo* **TSmx-a** they are positioned away (see Figs. 4 and 5). Consequently, this disposition at the *endo* **TSmn-a** favours the electrostatic interactions between nucleophilic and electrophilic frameworks with respect to the *exo* **TSmx-a**, thus justifying the preference for the *endo* stereoselectivity in the 32CA reaction between AY **11a** and NS **7**.

3.4 ELF topological analysis of the formation processes of the new C–C single bonds

Finally, in order to confirm the *pdr-type* reactivity of AYs **11a**,**b** and to understand the C–C single bond formation processes along the polar 32CA reactions of AYs **11a**,**b** with NS **7**, an ELF topological analysis of the stationary points, as well as of the most relevant points involved in the formation of the new C–C single bonds along the IRC associated with the most favourable *meta/endo/anti* reaction channel of the 32CA reaction involving methyl-substituted AY **11b**, is carried out. A BET procedure was used for the selection of

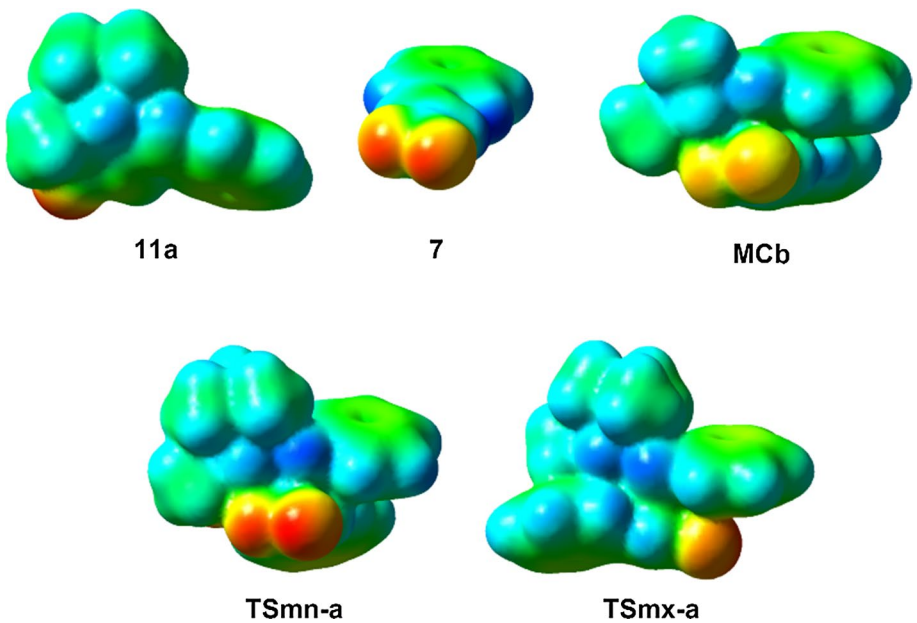

Fig. 5 MPWB1 K/6-31G(d) MEPs of AY **11a**, NS **7**, the *meta* regio isomeric TSs involved in the 32CA reaction between them and **MCb**

the mentioned points (those defining the phases in which the bond formation takes place and those defining the previous ones). The complete ELF analysis is given in the Supplementary Material.

Some appealing conclusions can be drawn from this ELF topological analysis: (1) formation of the new C1–C5 and C3–C4 single bonds takes place at C–C distances of ca. 2.02 and 2.10 Å, respectively, through the C-to-C coupling of two C1 and C5 *pseudoradical* centres (see Fig. 6); (2) formation of the first C1–C5 single bond involves the most nucleophilic centre of AY **11b**, the C1 carbon, and the most electrophilic centre of NS **7**, in agreement with the previous analysis of the Parr functions (see Sect. 3.2); (3) formation of the two C–C single bonds is asynchronous, in agreement with the previous geometry analysis (see Sect. 3.3.1); (4) formation of the second C3–C4 single bond takes place once the first one has been completed by up to 89.8%, characterising a non-concerted *two-stage one-step* mechanism [56]; (5) while the C1 and C3 *pseudoradical* centres are already present at AY **11b**, the C4 and C5 ones are created along the reaction progress after the rupture of the C4–C5 double bond of NS **7**, thus confirming the *pdr-type* mechanism of this 32CA reaction; (6) while the AY C1 *pseudoradical* participates more in the formation of the first C1–C5 single bond than the C5 one, the C4 *pseudoradical* created at the NS framework along the reaction progress contributes more to the formation of the second C3–C4 single bond than the C3 *pseudoradical* already present at AY **11b**; (7) as the only topological change at **TSmn-b** with respect to the ELF topological characteristics of **MCmn-b** is the disappearance of one of the two monosynaptic basins that characterise the C3 *pseudoradical* centre, the activation enthalpy associated with **TSmn-b** relative to **MCmn-b**, 2.5 kcal·mol^{-1}, can be mainly associated with the energy cost demanded for the depopulation of the C3 *pseudoradical* centre as well as the loss of the planar sp^2 hybridisation of the C3 carbon required for the formation of the new C3–C4 single bond; (8) unlike polar Diels–Alder reactions and polar *zw-type* 32CA reactions in which the GEDT favours the bonding changes at the reagents, i.e. the rupture of the double bonds, the high GEDT taking place at **TSmn-b**, 0.27e, does not favour the rupture of the C4–C5 double bond of the NS framework because the electron density coming from the GEDT process is disseminated almost equally between the nitro and phenyl substituents. This fact suggests that the low activation enthalpy associated with **TSmn-b** is not the consequence of a GEDT associated with a polar process, but of the stabilising non-covalent and electrostatic interactions already present at **MCmn-b** (see Section S1 in the Supplementary Material); and (9) the molecular mechanism of this 32CA reaction can be considered a [2n + 2τ] mechanism in which only two non-bonding electrons of AY **11b** and two electrons of the τ bond of NS **7** are involved.

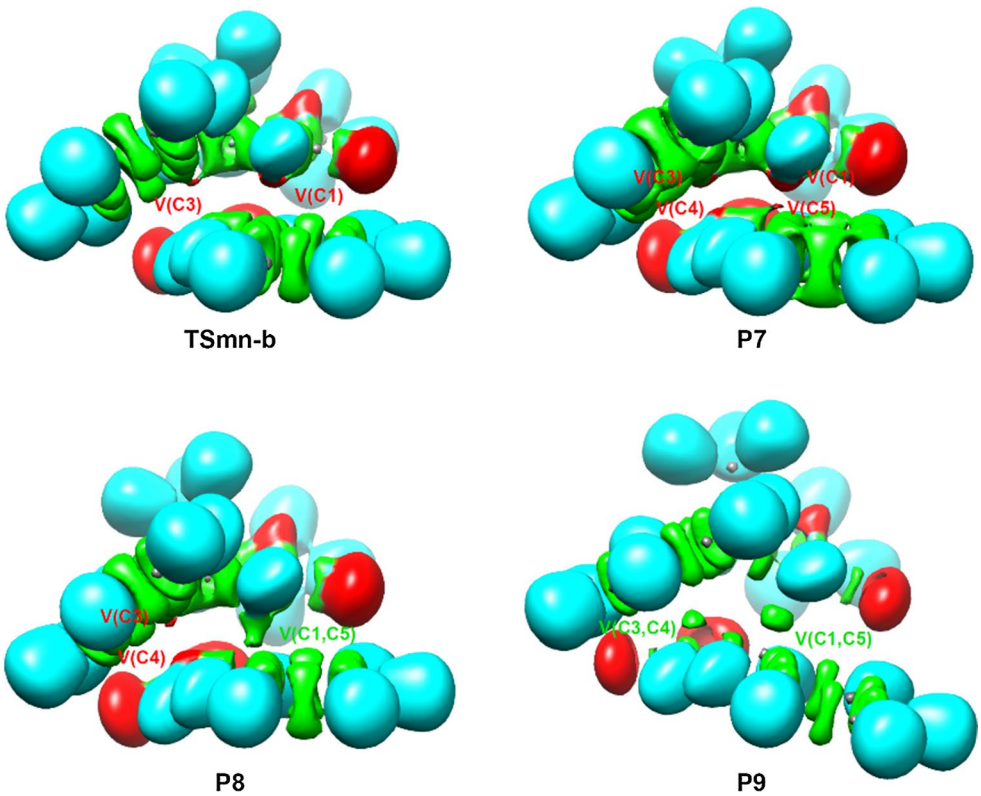

Fig. 6 ELF localisation domains of **TSmn-b** and the points of the IRC **P7**–**P9** defining *Phases VIII–X* involved in the formation of the new C1–C5 and C3–C4 single bonds along the polar *pdr-type* 32CA reaction between AY **11b** and NS **7**, represented at iso surface values of ELF = 0.71, 0.65, 0.69 and 0.80, respectively

4 Conclusions

The molecular mechanism and selectivity of the 32CA reaction of AY **11a** with NS **7** have been studied within the MEDT using DFT methods at the MPWB1K/6-31G(d) computational level. To this end, a methyl-substituted AY **11b** has been employed as a reduced model of the experimental AY **11a** [17].

ELF topological analysis of the electronic structure of AY **11b** indicates that this TAC has a *pseudodiradical* electronic structure that enables its participation in *pdr-type* 32CA reactions. Analysis of the CDFT global reactivity indices allows classifying AYs **11a,b** as strong nucleophiles and NS **7** as a strong electrophile. The presence of the *t*-Bu group of AY **11a** only increases slightly the nucleophilicity of the AY, thus expecting a similar reactivity for both AYs. In addition, analysis of the Parr functions permits to predict a total C1–C5 regioselectivity.

The *pdr-type* 32CA reactions of AYs **11a** and **11b** with NS **7** present low activation enthalpies, 2.5 and 4.1 kcal·mol^{-1}, respectively, and are irreversible, favouring kinetically the formation of pyrroloimidazoles **12n** generated from the *meta* regioisomeric, *endo* stereoisomeric and *anti* diastereofacial approach modes. While a *meta endo/exo* product mixture is kinetically expected in the reaction involving methyl-substituted AY **11b**, the *meta/endo* product is obtained as the single product in the reaction involving *t*-Bu substituted AY **11a**, in great agreement with the experimental observations.

The geometries of the TSs suggest an asynchronous bond formation processes in which the C1–C5 bond formation is more advanced than the C3–C4 one. In addition, the geometries point out the presence of O···H hydrogen bonds between one of the oxygen atoms of the nitro group of NS**7** and the C1–H or H6 hydrogens of AYs**11a**,**b**, which are confirmed by NCI and QTAIM topological analyses.

The MEPs of the *meta* TSs involved in the reaction of AY **11a** with NS **7** reveal that the disposition of the C3–H and H6 hydrogens above the electron-withdrawing nitro group at the *endo* **TSmn-a** favours the electrostatic interactions between both nucleophilic and electrophilic frameworks with respect to the *exo* **TSmx-a**, thus justifying the preference for the *endo* stereoselectivity in the 32CA reaction between AY **11a** and NS **7**.

The presence of such non-covalent interactions, as well as additional electrostatic and dipolar interactions at MCs and TSs supports their relevant role in the reaction rate of these polar *pdr-type* 32CA reactions, rather than the GEDT associated with a polar process.

Finally, ELF topological analysis of the C–C bond formation processes indicates that formation of the new C–C single bonds takes place at C–C distances of ca. 2.0–2.1 Å through the C-to-C coupling of two *pseudoradical* carbon centres. While the C1 and C3 *pseudoradical* centres are already present at AYs **11a**, **b**, the C4 and C5 ones must be created along the reaction progress from the rupture of the C4–C5 double bond of NS **7**. This ELF topological analysis allows characterising the molecular mechanism of the *pdr-type* 32CA reactions of AYs **11a**,**b** with NS **7** as a non-concerted *two-stage one-step* mechanism [56]. Moreover, considering the number and nature of electrons involved in the formation of the two new C–C single bonds, these 32CA reactions can be electronically classified as a [2n + 2τ] process in which only two non-bonding electrons of AY **11b** and two electrons of the τ bond of NS **7** are involved.

5 Supplementary material

Analysis of the strong stabilities of **MCb** and **TSmn-b**. ELF topological analysis of the formation of the new C–C single bonds along the most favourable *meta/endo/anti* reaction channel of the 32CA reaction involving methyl-substituted AY **11b**. Theoretical background of ELF, BET, QTAIM and NCI. Tables with: (1) gas phase MPWB1K/6-31G(d) and MPWB1K/6-311G(d,p)//MPWB1K/6-31G(d) total and relative energies of the stationary points involved in the *anti* diastereoisomeric pathways associated with the 32CA reaction of AY **11b** with NS **7** and MPWB1 K/6-31G(d) total and relative energies of those involved in the *meta/anti* pathways of the 32CA reaction with AY **11a**; (2) MPWB1 K/6-31G(d) thermodynamic data computed at 110 °C and 1 atm in toluene of the stationary points involved in the *anti* diastereoisomeric pathways associated with the 32CA reaction between AY **11b** and NS **7** and in the *meta/anti* pathways of the 32CA reaction with AY **11a**; (3) valence basin populations calculated from the ELF of IRC points defining the eleven phases characterising the molecular mechanism of the polar *pdr-type* 32CA reaction between AY **11b** and NS **7**. MPWB1K/6-31G(d) computed total energies and Cartesian coordinates in gas phase of all the structures.

Reference

1. Coura JR, De Castro SL (2002) Mem Inst Oswaldo Cruz 97:3
2. Franchetti P, Marchetti LS, Cappaellaci JA, Yalowitz HN, Jayaram BM, Glodstein M, Grafantini A (2001) Bioorg Med Chem Lett 11:67
3. Rizk A-FM (1999) In: Rizk A-FM (ed) Naturally occurring pyrrolizidine alkaloids. CRC Press Inc., Boca Raton
4. Xue J, Zhang Y, Wang X-I, Fun HK, Xu JH (2000) Org Lett 2:2583
5. Lin GQ, Li YM, Chan ASC (2001) Principles and applications of asymmetric synthesis. John Wiley & Sons, New York
6. Carrieri A, Muraglia M, Corbo F, Pacifico C (2009) Eur J Med Chem 44:1477

7. Gabrielsen M, Kurczab R, Siwek A, Wolak M, Ravna AW, Kristiansen K, Kufareva I, Abagyan R, Nowak G, Chilmonczyk Z, Sylte I, Bojarski AJ (2014) J Chem Inf Model 54:933
8. Padwa A (1984) (Ed.) 1,3-Dipolar Cycloaddition Chemistry, vols. 1 and 2, Wiley/Interscience, New York
9. Pandey G, Banerjee P, Gadre SR (2006) Chem Rev 106:4484
10. Domingo LR (2016) Molecules 21:1319
11. Domingo LR, Emamian SR (2014) Tetrahedron 70:1267
12. Domingo LR, Ríos-Gutiérrez M (2017) Molecules 22:750
13. Domingo LR, Ríos-Gutiérrez M, Pérez P (2016) Tetrahedron 72:1524
14. Domingo LR, Chamorro E, Pérez P (2010) Lett Org Chem 7:432
15. Domingo LR, Aurell MJ (1050) P. Pérez. Tetrahedron 2015:71
16. Sobhi C, Khorief Nacereddine A, Djerourou A, Ríos-Gutiérrez M (2017) L R Domingo J Phys Org Chem 30:6
17. Zhang X, Wang X, He Y, Liu Y, Liu J, Shi J (2016) Tetrahedron Lett 57:1143
18. Nacereddine AK, Layeb H, Chafaa F, Yahia W, Djerourou A, Domingo LR (2015) RSC Adv 5:64098
19. Nacereddine AK, Sobhi C, Djerourou A, Ríos-Gutiérrez M, Domingo LR (2015) RSC Adv 5:99299
20. Ríos-Gutiérrez M, Chafaa F, Nacereddine AK, Djerourou A, Domingo LR (2016) J Mol Graph Model 70:296
21. Zhao Y, Truhlar DG (2004) J Phys Chem A 108:6908
22. Hehre WJ, Radom L, Schleyer PVR, Pople JA (1986) Ab Initio molecular orbital theory. Wiley, New York
23. Schlegel HB (1982) J Comput Chem 3:214–218
24. Schlegel HB (1994) In: Yarkony DR (ed) Modern electronic structure theory. World Scientific Publishing, Singapore
25. Fukui K (1970) J Phys Chem 74:4161
26. González C, Schlegel HB (1990) J Phys Chem 94:5523
27. González C, Schlegel HB (1991) J Chem Phys 95:5853
28. Tomasi J, Persico M (1994) Chem Rev 94:2027
29. Simkin BY, Sheikhet I (1995) Quantum chemical and statistical theory of solutions-computational approach. Ellis Horwood, London
30. Cances E, Mennucci B, Tomasi J (1997) J Chem Phys 107:3032
31. Cossi M, Barone V, Cammi R, Tomasi J (1996) Chem Phys Lett 255:327
32. Barone V, Cossi M, Tomasi J (1998) J Comput Chem 19:404
33. Geerlings P, De Proft F, Langenaeker W (2003) Chem Rev 103:1793
34. Domingo LR, Ríos-Gutiérrez M, Pérez P (2016) Molecules 21:748
35. Domingo LR (2014) RSC Adv 4:32415
36. Reed AE, Weinstock RB, Weinhold F (1985) J Chem Phys 83:735
37. Reed AE, Curtiss LA, Weinhold F (1988) Chem Rev 88:899
38. Frisch MJ et al (2009) Gaussian 09, revision A.02. Gaussian Inc, Wallingford
39. Becke AD, Edgecombe KE (1990) J Chem Phys 92:5397
40. Bader RFW (1990) Atoms in molecules. A quantum theory. Claredon Press, Oxford
41. Johnson ER, Keinan S, Mori-Sanchez P, Contreras-García J, Cohen J, Yang AW (2010) J Am Chem Soc 132:6498
42. Noury S, Krokidis K, Fuster F, Silvi B (1999) Comput Chem 23:597
43. Lu T, Chen F (2012) J Comput Chem 33:580
44. Contreras-García J, Johnson ER, Keinan S, Chaudret R, Piquemal J-P, Beratan DN, Yang W (2011) J Chem Theory Comput 7:625
45. Krokidis K, Noury S, Silvi B (1997) J Phys Chem A 101:7277–7282
46. Parr RG, Pearson RG (1983) J Am Chem Soc 105:7512
47. Parr RG, Yang W (1989) Density functional theory of atoms and molecules. Oxford University Press, New York
48. Parr RG, Von Szentpaly L, Liu S (1922) J Am Chem Soc 1999:121
49. Domingo LR, Chamorro E, Pérez P (2008) J Org Chem 73:4615
50. Domingo LR, Pérez P (2011) Org Biomol Chem 9:7168
51. Domingo LR, Aurell MJ, Pérez P, Contreras R (2002) Tetrahedron 58:4417
52. Jaramillo P, Domingo LR, Chamorro E, Pérez P (2008) J Mol Struct 865:68
53. Domingo LR, Sáez JA (2009) Org Biomol Chem 7:3576
54. Domingo LR, Ríos-Gutiérrez M (2017) P. Pérez. Tetrahedron 73:1718
55. Domingo LR, Pérez P, Sáez JA (2013) RSC Adv 3:1486
56. Domingo LR, Saéz JA, Zaragozá RJ, Arnó M (2008) J Org Chem 73:8791